



Universiteit
Leiden
The Netherlands

Catalytic allylation of phenols : chloride-free route towards epoxy resins

Rijn, J.A. van

Citation

Rijn, J. A. van. (2010, September 14). *Catalytic allylation of phenols : chloride-free route towards epoxy resins*. Retrieved from <https://hdl.handle.net/1887/15943>

Version: Corrected Publisher's Version

License: [Licence agreement concerning inclusion of doctoral thesis in the Institutional Repository of the University of Leiden](#)

Downloaded from: <https://hdl.handle.net/1887/15943>

Note: To cite this publication please use the final published version (if applicable).

3

[RuCp(PP)]⁺-catalyzed allylation of phenols: a gem-dialkyl-type effect induces high selectivity for O-allylation

Abstract

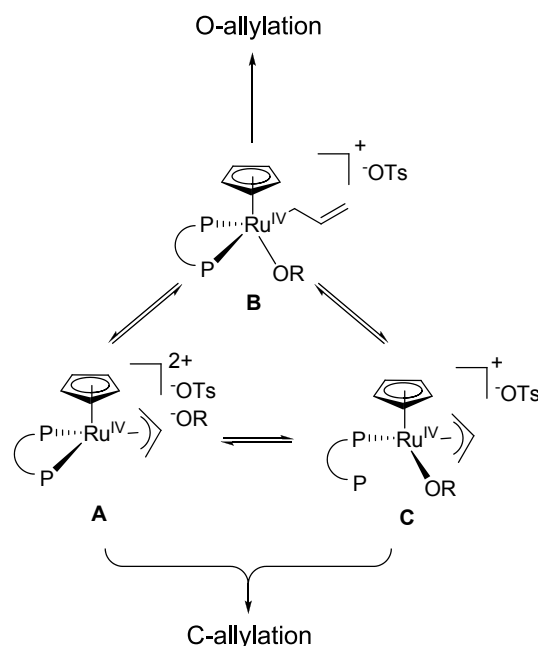
It appears that catalysts containing bidentate phosphine ligands having geminal dialkyl substituents at the central atom of a C₃-bridging group of the phosphine ligand are highly selective for O-allylation of phenol with allyl alcohol; apparently the presence of the substituents efficiently blocks the competitive and thermodynamically more favorable pathway to C-allylation. It appears that the electronic and structural properties of the Ru(II) precursor complexes in the solid state do not differ significantly from those of complexes containing unsubstituted analogous ligands, while the resulting catalysts show a vastly different catalytic performance. The results suggest that the geminal dialkyl substitution at the central carbon of the C₃-bridge of the ligand primarily leads to an increased kinetic stability of the bidentate chelate under reaction conditions, such as in the proposed intermediate [Ru(IV)Cp(diphosphine)(allyl)]²⁺ complexes. This implies that the high kinetic stability of the diphosphine chelate bound to Ru blocks the pathway to the thermodynamically favored C-allylation product. The results provide an interesting example in which the application of the geminal dialkyl substitution in the bridge of a bidentate ligand serves as a diagnostic tool to probe the nature of the selectivity-determining step in a catalytic pathway in homogeneous catalysis.

3.1 Introduction

Selective O-allylation of phenols is a highly desired reaction in the development of an environmentally benign synthesis of epoxy resins on an industrial scale.¹ Catalytic O-allylation of phenols is most frequently reported using allylating agents with good leaving groups such as allyl chloride or allyl acetate and stoichiometric amounts of base are added to induce good selectivity;²⁻⁴ these processes thus all result in stoichiometric saline waste. From an atom-efficiency point of view it would be desirable to use allyl alcohol as allylating agent, forming only water in the process. An example of selective O-allylation of phenol with allyl alcohol was demonstrated using a palladium catalyst in the presence of stoichiometric amounts of the base $(\text{Ti}(\text{OiPr})_4)$.⁵ In an industrial application this would lead to a vast quantity of Ti-salt waste, which is clearly undesired. In the absence of the Ti-salt, however, such a catalytic system leads to C-allylation.⁶ Also with the Ru(IV) catalyst precursor described by Pregosin and co-workers,⁷ phenols are exclusively C-allylated.

In Chapter 2, a $[\text{RuCp}(\text{diphosphine})]$ -based catalytic system is described that catalyzes both O- and C-allylation of phenols with allyl alcohol, without the need of any stoichiometric amounts of additives. It was shown that formation of O-allylated products is equilibrium limited, while C-allylated products are produced irreversibly as the thermodynamically favored product. It was also found that the addition of a catalytic quantity of a Brønsted acid has a major effect on the rate of allylation as well as the course of the reaction. A triplet of isomeric $\text{Ru(IV)Cp(PP)(allyl)(OR)(OTs)}$ intermediates formed after oxidative addition of either allyl alcohol or allyl phenyl ether at $[\text{Ru(II)Cp(PP)}](\text{OTs})$ are believed to play a key role in determining the selectivity of the allylation reaction (Scheme 3.1). As the desired product is formed in an equilibrium reaction, it implies that it is not useful to discuss this reaction in terms of yields. In an industrial process, however, this type of reaction may be applied with recycling of the reactants, for which especially high selectivity is important.

It is thought that, next to the 18-electron σ -allyl species **B**, both π -allyl species **A** and **C** can be reversibly accessed. To prevent a 20-electron species, it is proposed that either the RO^- anion is expelled from the coordination sphere (**A**), or that phosphine dissociation will occur (**C**). From the observed catalyst structure- performance relationship of the Ru catalysts it is concluded that the availability of space around the ruthenium center is an important factor in determining the course of the allylation reaction (Chapter 2). It is suggested that it could be species **C** that provides sufficient space at the Ru(IV) center to accommodate the apparently



Scheme 3.1. Proposed intermediates in the catalytic allylation of phenol with allyl alcohol.

space-demanding transition state towards C-allylation, while competitive reductive elimination from species **B** would produce the desired allyl ether (Chapter 2).

Dissociation of one phosphorus donor of the bidentate phosphine ligand could thus be a possible event to create the necessary space at the ruthenium center to open up the pathway towards C-allylation. Alternatively, the sterics of the chelating diphosphine ligand itself – and not its partial dissociation – could also be a crucial factor determining the competition between O-allylation and C-allylation involving species of type **A** and **B**. In the present work, experiments are described that will allow us to discriminate between either ligand dissociation or its sterical demands as a chelating ligand, in the crucial selectivity-determining step in the catalytic cycle. A series of complexes with chelating bidentate phosphine ligands with a focus on backbone variation (Figure 3.1) was tested for their activity and selectivity in the allylation of phenol with allyl alcohol. The ligands, with bridging groups ranging from C₁ to C₃, all have substitution on the ligand backbone and were selected to investigate if ligand dissociation and/or the ligand sterical demands determine selectivity in this reaction by comparing them with their unsubstituted analogues (Chapter 2).

3.2 Results and discussion

3.2.1 Synthesis

The catalyst precursor complexes [RuCpCl(PP)] with the ligands shown in Figure 3.1 were synthesized using a procedure reported in Chapter 2. It was found that formation of the

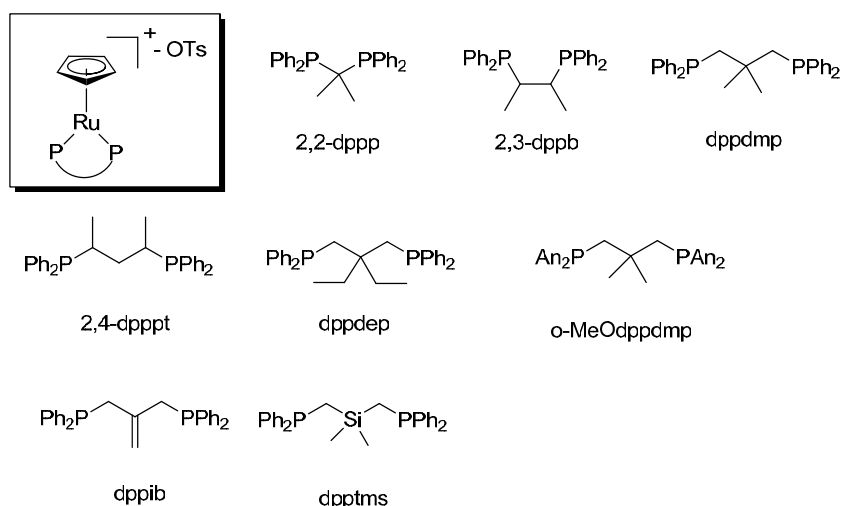


Figure 3.1. Schematic overview of the catalytic ruthenium complexes with the employed bidentate phosphine ligands and their abbreviations (An = *o*-anisyl).

complexes with ligands containing a substituted bridge generally requires longer reaction times than those with unsubstituted ligands (16 vs 6 hours). A striking feature of the new complexes is their high stability in solution in air. Whereas [RuCpCl(PP)] complexes of diphosphines with unsubstituted alkylene bridges rapidly decompose in solution when exposed to air, these novel complexes are stable for several weeks on the bench and crystals can even be grown in air. The yields of the syntheses were high and all complexes have been characterized by elemental analysis, $^1\text{H-NMR}$ and $^{31}\text{P-NMR}$ spectroscopy. In the complexes with *geminal* substitution, the two alkyl substituents on the central carbon in the bridge are non-equivalent with respect to the Cp ring; separate signals are detected in $^1\text{H-NMR}$.

The phosphorus resonances of the complexes with the *geminal* disubstituted C_3 -ligands are very similar to that of unsubstituted complexes, i.e. [RuCpCl(dppp)] and [RuCpCl(dppdmp)] both show a $^{31}\text{P-NMR}$ resonance around +40 ppm, indicating that the ligand binding properties to Ru(II) in these complexes hardly change by substitution at the central carbon of the C_3 -bridging group. Also the complex [RuCpCl(dppib)], in which dppib can be viewed as a special geminally substituted C_3 -diphosphine ligand, shows a similar resonance in $^{31}\text{P-NMR}$ (43.0 ppm). On the other hand, for [RuCpCl(2,4-dpppt)] (1,3-disubstitution of the C_3 -bridge) the $^{31}\text{P-NMR}$ spectrum shows a significant shift (to 51.8 ppm). Geminal dialkyl substitution of the ligand with a C_1 -bridging group has a significant effect on the ligand binding properties, as indicated by the $^{31}\text{P-NMR}$ chemical shift of 43.0 ppm for [RuCpCl(2,2-dppp)] vs 15.7 ppm for [RuCpCl(dppm)]. Alkyl substitution at a C_2 -bridging group leads to a less dramatic effect on the ^{31}P NMR resonances: i.e. 86.0 ppm for [RuCpCl({S,S}-2,3-dppb)] versus 80.1 ppm for [RuCpCl(dppe)].

3.2.2 Crystal structures

Crystals of [RuCpCl(dppdep)], [RuCpCl(dppdmp)], [RuCpCl(dpptms)], [RuCpCl(*o*-MeOdppdmp)] and [RuCpCl(2,2-dppp)] were obtained by slow diffusion of n-hexane into solutions of the complexes in toluene. Selected bond distances and angles are listed in Table 3.1.

The asymmetric units of [RuCpCl(*o*-MeOdppdmp)] and [RuCpCl(2,2-dppp)] contain two independent molecules; distances and angles are given in Table 3.1 for only one of the

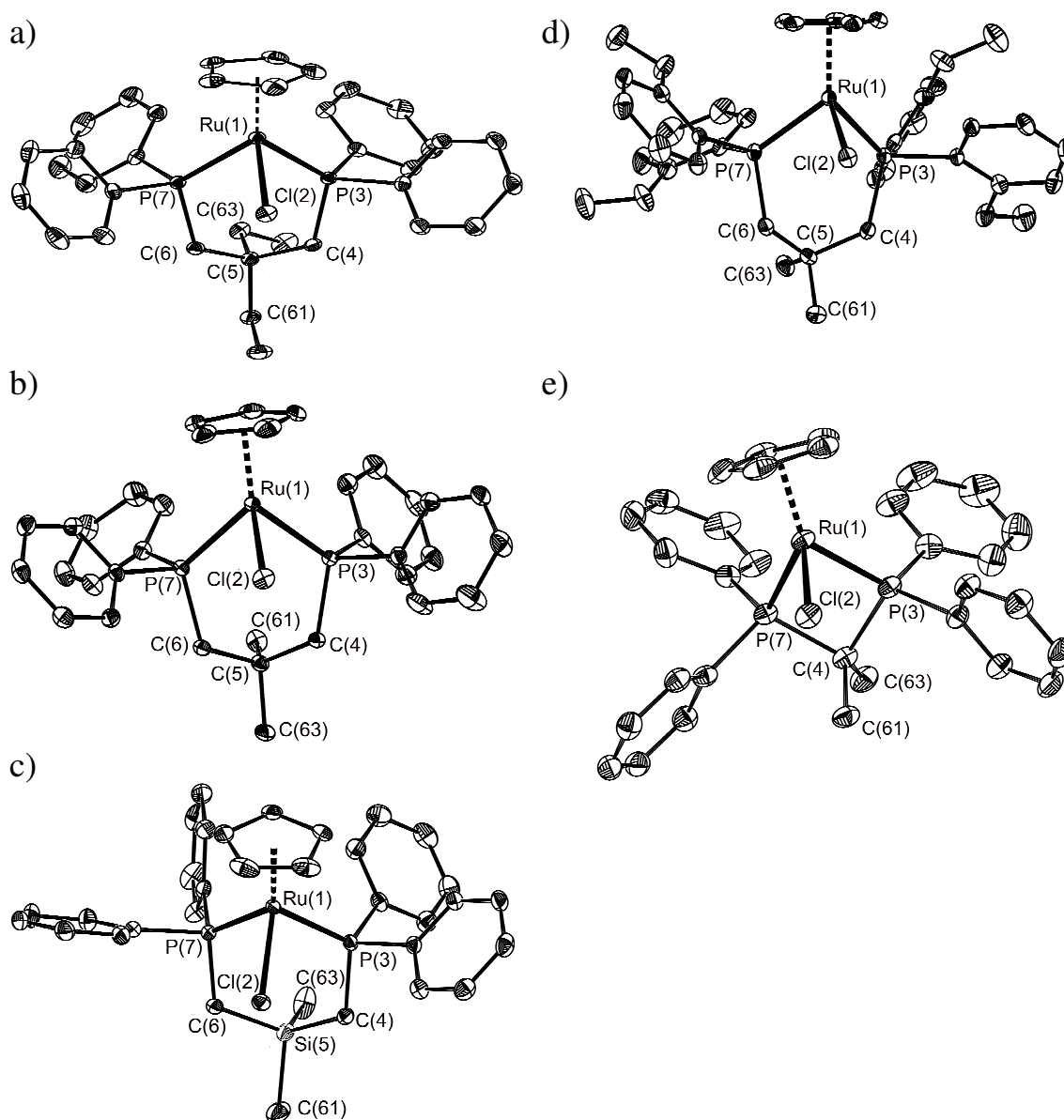


Figure 3.2. Displacement ellipsoid plots (50% probability level) of one formula unit of a) [RuCpCl(dppdep)], b) [RuCpCl(dppdmp)], c) [RuCpCl(dpptms)], d) [RuCpCl(*o*-MeOdppdmp)] and e) [RuCpCl(2,2-dppp)]. For [RuCpCl(dppdep)], the minor component of the disordered Cp ligand and the lattice disordered toluene molecule are omitted for clarity. For [RuCpCl(*o*-MeOdppdmp)] and [RuCpCl(2,2-dppp)], only one of the two independent molecules is shown. H-atoms are omitted for the sake of clarity.

Table 3.1. Selected bond lengths (Å) and angles (°) for the complexes [RuCpCl(dppdep)], [RuCpCl(dppdmp)], [RuCpCl(dpptms)], [RuCpCl(*o*-MeOdppdmp)] and [RuCpCl(2,2-dppp)].

	[RuCpCl (dppdep)]	[RuCpCl (dppdmp)]	[RuCpCl (dpptms)]	[RuCpCl(<i>o</i> - MeOdppdmp)]	[RuCpCl(2,2- dppp)]
<i>Bond distances (Å)</i>					
Ru(1)-Cl(2)	2.4370(5)	2.4443(4)	2.4384(3)	2.4512(9)	2.4259(8)
Ru(1)-P(3)	2.2820(5)	2.2984(4)	2.2749(4)	2.2891(10)	2.2890(6)
Ru(1)-P(7)	2.2817(4)	2.2668(4)	2.3028(3)	2.2619(10)	2.2620(6)
Ru(1)-Cp	1.852(2)	1.8608(8)	1.8524(7)	1.8494(18)	1.867(2)
<i>Angles (°)</i>					
P(3)-Ru(1)-P(7)	91.946(16)	92.078(15)	93.869(13)	91.09(3)	71.54(2)
P(3)-Ru(1)-Cl(2)	84.29(2)	82.435(14)	87.419(12)	87.34(3)	91.08(2)
P(7)-Ru(1)-Cl(2)	83.75(2)	85.078(14)	88.118(12)	87.10(3)	95.41(2)
C(4)-C(5)-C(6)	111.31(13)	111.19(12)	-	114.7(3)	-
C(4)-Si(5)-C(6)	-	-	110.29(6)	-	-
P(3)-C(4)-P(7)	-	-	-	-	89.37(9)
C(61)-C(5)-C(63)	108.89(14)	108.71(13)	-	106.8(3)	-
C(61)-Si(5)-C(63)	-	-	108.71(9)	-	-
C(61)-C(4)-C(63)	-	-	-	-	109.35(19)

independent molecules as the structural parameters are very similar. The displacement ellipsoid plots of [RuCpCl(dppdep)], [RuCpCl(dppdmp)], [RuCpCl(dpptms)], [RuCpCl(*o*-MeOdppdmp)] and [RuCpCl(2,2-dppp)] are shown in Figure 3.2.

The distances of the ruthenium center to the cyclopentadienyl group, the phosphorus atoms and the chloride anion are quite similar for all five compounds and are comparable to related ruthenium complexes (Chapter 2).⁸⁻¹¹ The effects of the backbone substituents on the overall solid state structure are rather small; especially the bite angle of the diphosphine ligand hardly changes (92.591(15)° and 91.09(3)° for [RuCpCl(*o*-MeOdppp)] (Chapter 2) and [RuCpCl(*o*-MeOdppdmp)], respectively). Also no significant difference in the angle C(4)-C(5)-C(6) between these two compounds is present (115.32(14)° vs 114.7(3)°). When the substituents are changed from methyl to ethyl groups, a change in angles is foreseen; however, for [RuCpCl(dppdep)] and [RuCpCl(dppdmp)] neither the bite angle (91.946(16)° vs 92.078(15)°) nor the C(4)-C(5)-C(6) angle (111.31(13)° vs 111.19(12)°) are significantly changed.

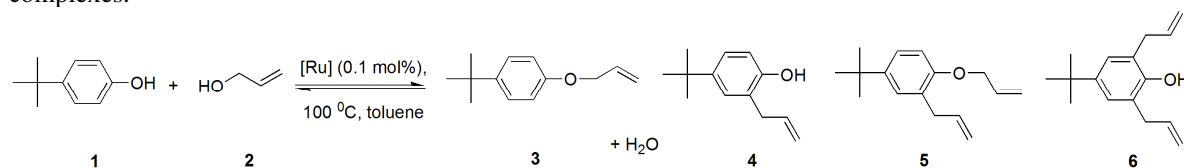
Also for C₁-bridged complexes, where the bite angle is expected to be more directly influenced by introduction of substituents, the difference between [RuCpCl(dppm)]⁹ and the dimethyl-substituted [RuCpCl(2,2-dppp)] is negligible (72.07(2)° vs 71.60(2)°). A potential angle compression due to the presence of the (geminal) substituents is thus not reflected in the solid-state structures of the Ru(II) complexes.

3.2.3 Catalysis

The catalytic activity of the ruthenium complexes with methyl substituents on the ligand backbone in the allylation of 4-*tert*-butylphenol with allyl alcohol was investigated; the results are shown in Table 3.2. A catalyst loading of 0.1 mol% was used at a reaction temperature of 100 °C. Apart from the desired O-allylated product **3**, the undesired C-allylated products **4-6** are formed, as reported in Chapter 2. The results of the catalytic experiments using the complexes with unsubstituted bidentate phosphine ligands dppm, dppe and dppp are listed in entries 2, 4 and 7 for comparison.

It has been reported in Chapter 2 that the use of both dppm and dppe as the ligand results in very low selectivity for O-allylation (entries 2 and 4), but with completely different activity. The use of dppm yields a catalyst with low activity, while the use of dppe yields a highly active catalyst, resulting in the formation of almost exclusively C-allylated products with high rate. Geminal substitution of the C₁-bridged ligand in [RuCp(2,2-dppp)](OTs) (entry 1) results in an increase in the rate of the reaction as well as the selectivity for O-allylation. Vicinal disubstitution of the C₂-backbone ligand in [RuCp(2,3-dppb)](OTs) (entry 3), however, seems to have no effect on either rate or selectivity (cf entries 3 and 4). On the other hand, complexes with dialkyl substituted C₃-backbones, i.e. [RuCp(dppdmp)](OTs) (entry 5) and [RuCp(2,4-dpppt)](OTs) (entry 6), show a much higher selectivity towards O-allylated product **3** (up to 87%), combined with a somewhat lower catalyst activity, compared to the complex [RuCp(dppp)](OTs) (entry 7). The effect of 1,3-dimethyl substitution of the C₃ backbone for the 2,4-dpppt ligand might perhaps not be too surprising as the methyl

Table 3.2. Reaction of 4-*tert*-butylphenol (**1**) with allyl alcohol (**2**) catalyzed by different [RuCp(PP)]⁺ complexes.^a



entry	[RuCp(PP)] (OTs) PP =	conversion of 1 (%)	selectivity for (%)	
			3	4-6
1	2,2-dppp	44	27	73
2 ^b	dppm	21	2	98
3	2,3-dppb	74	4	96
4 ^b	dppe	72	4	96
5	dppdmp	30	87	13
6	2,4-dpppt	25	86	14
7 ^b	dppp	53	44	56

^a Reaction conditions: ratio 4-*tert*-butylphenol/allyl alcohol/[RuCpCl(PP)]/AgOTs = 1000/1000/1/2, toluene, 100 °C, 3 h.

^b Results taken from Chapter 2

Table 3.3. Reaction of 4-*tert*-butylphenol (**1**) with allyl alcohol (**2**) catalyzed by different [RuCp(PP)]⁺ complexes.^a

entry	[RuCp(PP)] (OTs) PP =	conversion of 1 (%)				selectivity for (%)							
		0.5 h	1 h	3 h	6 h	0.5 h		1 h		3 h		6 h	
						3	4-6	3	4-6	3	4-6	3	4-6
1	dppdmp	2	7	30	63	>99	0	>99	0	87	13	82	18
2	dppdep	1	4	20	31	>99	0	>99	0	90	10	88	12
3	<i>o</i> -MeOdppdmp	0	0	9	17	-	-	-	-	>99	0	99	1
4	dppib	0	4	26	46	-	-	>99	0	85	15	63	37
5	dpptms	0	2	20	41	-	-	>99	0	99	1	84	16
6 ^b	dppp	24	42	53	70	80	20	70	30	44	56	27	73

^a Reaction conditions: ratio 4-*tert*-butylphenol/allyl alcohol/[RuCpCl(PP)]/AgOTs = 1000/1000/1/2, toluene, 100 °C

^b results taken from Chapter 2

substituents adjacent to phosphorous will lead to significantly altered stereo-electronic ligand binding characteristics of the diphosphine ligand, as is in fact indicated by the ³¹P-NMR data. The most intriguing observation from Table 3.2 is that the selectivity for O-allylation of the complex [RuCp(dppdmp)](OTs) (entry 5) compared to [RuCp(dppp)](OTs) is increased in a major way. This is a remarkable observation, as both the ³¹P-NMR data and the X-ray structures of these Ru(II) catalyst precursors suggest that these ligands impose a very similar stereo-electronic coordination environment at the ruthenium center. Therefore, the catalytic performance of [RuCp(dppdmp)](OTs) and RuCp complexes of other ligands with *geminal* substitution on the central atom of C₃-backbone ligands shown in Figure 3.1 were studied in more detail. Conversions and selectivities as a function of reaction time are shown in Table 3.3.

The complex [RuCp(dppdmp)](OTs) (entry 1) shows a remarkably steady activity while maintaining a high selectivity towards product **3** after longer reaction times. Even after six hours and more than 60% conversion the selectivity for the O-allylated product is relatively high (82%). This is in sharp contrast with the performance of the unsubstituted analogue [RuCp(dppp)](OTs) (entry 6), which rapidly forms increased amounts of C-allylated products over time. Increasing the bulk on the C₃ backbone from methyl to ethyl groups in [RuCp(dppdep)](OTs) (entry 2) results in slightly higher selectivities, but with a somewhat decreased activity of the catalyst. Introduction of *ortho*-methoxy groups on the phenyl rings in [RuCp(*o*-MeOdppdmp)](OTs) (entry 3) results in lower activity compared to [RuCp(dppdmp)](OTs), but with a very high selectivity for O-allylation. For the catalyst with an isobutene bridging group (entry 4) the initial activity and selectivity are comparable to that of [RuCp(dppdmp)](OTs) (entry 1), but after longer reaction times the selectivity for O-allylation deteriorates. The introduction of a silicon atom in the central position of the bridge

Table 3.4. Reaction of 4-*tert*-butylphenol with allyl alcohol catalyzed by different complexes in presence of acid ^a

Entry	[RuCp(PP)](OTs)	conversion of 1 (%)			selectivity (%)					
		0.5 h	1 h	3 h	0.5 h		1 h		3 h	
	PP =				3	4-6	3	4-6	3	4-6
1	dppdmp	46	57	58	83	17	58	42	46	54
2	dppdep	44	58	71	>99	0	90	10	73	27
3	<i>o</i> -MeOdppdmp	41	42	48	95	5	95	5	95	5
4	dppib	74	74	78	9	91	2	98	2	98
5	dpptms	39	54	69	90	10	85	15	68	32
6 ^b	dppp	70	74	80	35	65	24	76	2	98

^a Reaction conditions: ratio 4-*tert*-butylphenol/allyl alcohol/[RuCpCl(PP)]/AgOTs/HOTs = 1000/1000/1/2/2, 100 °C.

^b Results taken from Chapter 2

in [RuCp(dpptms)](OTs) (entry 5) leads to a decrease in activity compared to entry 1, but with a slightly higher selectivity.

3.2.4 Acid effect

In Chapter 2 it has been reported that addition of catalytic quantities of a strong acid to RuCp(PP) catalyst systems, e.g. *p*-toluenesulfonic acid (HOTs), not only significantly increases the activity of the catalysts, but also affects the selectivity. The effect of acid on the activity and selectivity of the catalysts with the dialkyl substituted C₃ ligands was thus investigated in more detail; the results are presented in Table 3.4.

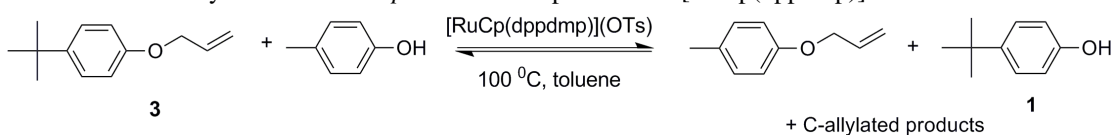
For [RuCp(dppdmp)](OTs) (entry 1, Table 3.4), in the presence of acid the conversion of **1** after 30 minutes is already higher than the conversion after 3 hours without acid (entry 1; Table 3.3). After longer reaction times selectivity towards **3** slowly deteriorates, but in a much lesser extent than observed for the unsubstituted analogue [RuCp(dppp)](OTs) (entry 6). Although conversion hardly increases between 1 and 3 hours, in this time span the selectivity changes, indicating that the catalyst is still active as an allylation catalyst. However, as the product **3** is now present in a higher concentration than allyl alcohol, the catalyst now converts **3** to the thermodynamically-favored products **4-6**. For the catalyst with the more bulky bridge-substituted ligand [RuCp(dppdep)](OTs) (entry 2), the increase in rate is even more pronounced, but the selectivity remains higher than that of [RuCp(dppdmp)](OTs). The catalyst [RuCp(*o*-MeOdppdmp)](OTs) in the absence of acid (entry 3; Table 3.3) is not very active, but in the presence of acid (entry 3) the activity is increased dramatically with excellent selectivity for O-allylation. The lifetime of this catalyst in the presence of acid, however, appears to be rather short, as after 30 minutes the conversion hardly increases. Catalyst stability was tested by adding a second batch of substrates **1** and **2** after three hours, and while all other catalysts converted this newly introduced batch in a similar manner as the

original batch, the $[\text{RuCp}(o\text{-MeOdpdpmp)](\text{OTs})$ did not show significant continued conversion. Degradation of the complex is thought to occur by cleavage of a methyl group from the anisyl ring, creating a strongly coordinating phenoxyl anion, for which there is precedence in literature.^{12,13} The catalyst $[\text{RuCp}(\text{dppib})](\text{OTs})$ (entry 4) in the presence of acid also shows a much higher activity, but the selectivity for O-allylation is decreased in a dramatic way and after three hours its performance is very similar to that of the non-substituted $[\text{RuCp}(\text{dppp})]^+$ (entry 6). Finally, for the catalyst with the dimethylsilane-bridged ligand $[\text{RuCp}(\text{dpptms})](\text{OTs})$ (entry 5) the activity and selectivity appear comparable to that of $[\text{RuCp}(\text{dppdep})](\text{OTs})$.

3.2.5 Transallylations

In Chapter 2, it has been shown that allyl ethers can also be activated at the ruthenium center. The transallylation activity has been used as a diagnostic test to investigate the reactivity of the catalysts for the conversion of **3** in the presence of *p*-cresol. The results of this investigation using $[\text{RuCp}(\text{dppdmp})](\text{OTs})$ as the catalyst are given in Table 3.5. Hardly any activity is observed in the absence of acid, but in the presence of acid the reaction reaches equilibrium within one hour, forming equal amounts of the allyl ethers of 4-*tert*-butylphenol and *p*-cresol. Only a small amount of C-allylated products is co-produced. These results thus indicate a strong co-catalytic role of protons in the oxidative addition of allyl phenyl ether, similar to that encountered in the activation of allyl alcohol. The results clearly show that trans-allylation of **3** with *p*-cresol proceeds with good selectivity when dppdmp is applied as the ligand. A considerably smaller loss to thermodynamically more favorable C-allylated products is observed compared to the catalyst with the ligand dppp (entry 3). This is consistent with the observations in the direct allylation of phenol with allyl alcohol (Table

Table 3.5. Transallylation of **3** with *p*-cresol in the presence of $[\text{RuCp}(\text{dppdmp})]^+$ ^a



entry	acid	conversion of 3 (%)	selectivity (%) ^b	
			O-allyl	C-allyl
1	-	~0	-	-
2	HOTs	64	86	14
3 ^c	HOTs	80	55	45

^a Reaction conditions: **3**/*p*-cresol/ $[\text{RuCpCl}(\text{dppdmp})]/\text{AgOTs}/(\text{HOTs}) = 1000/1000/1/2/(2)$, 100 °C, toluene, 1 h

^b O-allyl = total O-allylated products; C-allyl = total C-allylated products

^c $[\text{RuCpCl}(\text{dppp})]$ was used; taken from Chapter 2

3.3) and confirms the tremendous effect of the ligand choice in the selectivity determining step in the catalytic cycle.

3.2.6 *Kinetically stable chelate vs steric hindrance*

Moloy and co-workers^{14,15} have investigated the influence of substitution on the ligand backbone in reductive elimination reactions involving Pd and Pt complexes. Mul *et al.*¹⁶ have reported a surprising effect of geminal dialkyl substitution of C₃-bridged diphosphine ligands in Pd-catalyzed olefin-carbon monoxide copolymerization. As shown above, the *geminal* dialkyl substitution of ligand backbones also has a positive influence on the system of (diphosphine)Ru-catalyzed allylation of phenol, apparently by blocking the C-allylation pathway. It has been proposed in Chapter 2 that restricted coordination space at the Ru center is a crucial catalyst parameter to prevent C-allylation. The question arises how the geminal dialkyl substitution at the central carbon of a C₃-backbone can influence the coordination space at ruthenium.

From the NMR and X-ray data of the catalyst precursor Ru(II) complexes it is concluded that the stereo-electronic coordination properties of the ligands do not change significantly upon backbone substitution; it is therefore reasonable to assume that the same is true for the proposed catalytic Ru(IV) intermediates shown in Scheme 3.1. Since the substituents at the central carbon atom are directed away from the reactive center, a significant contribution to the immediate static steric environment is not expected, both in the Ru(II) and the Ru(IV) complexes. Thus, it is very likely that the stability of the chelate under reaction conditions is the prime factor discriminating the substituted from the unsubstituted ligand. The Ru(II)Cp complexes with the *geminal* substituted ligands are highly stable, even in solutions of different solvents in air over longer periods of time, whereas complexes of the bidentate phosphine ligands with unsubstituted bridges (dppm, dppe and dppp) are oxidized within a few hours.

Therefore, it is concluded that that it is the kinetically stable chelation of these ligands which is the major cause for the high selectivity of their ruthenium complexes for O-allylation, i.e. an effect similar in origin as the “*gem*-dialkyl effect” coined by Moloy *et al.*¹⁵ For diphosphine ligands with substituted backbones rotational freedom necessary for phosphine dissociation is severely limited; the equilibrium between the *gauche*- and *anti*-conformation (Figure 3.3), lies more towards the *gauche*-conformer where chelation takes place. Without substituents on the ligand backbone, the interactions are weak and rotation will be far less

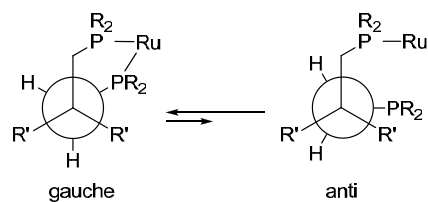


Figure 3.3. Schematic representation of the rotational restriction caused by *gem*-dialkyl substitution in a ruthenium diphosphine complex.

hindered. Introduction of additional substituents on the phenyl rings on the phosphorus atom as in $[\text{RuCp}(o\text{-MeOdppdmp})](\text{OTs})$ will decrease the rotational freedom even further.¹⁶ For a rigid ligand like dppib, which may be considered a special case of *gem*-disubstitution, rotational freedom is reduced due to the sp^2 hybridisation of the central carbon in the bridge. However, especially in the presence of acid, the catalyst with this ligand does not show a high selectivity towards O-allylation. It is proposed that the substitution causing rotational restriction and thereby selectivity for O-allylation decreases in the series $\text{dppdep} > \text{dppdmp} > \text{dppib} > \text{dppp}$.

The complex of the ligand with substitution pattern other than C_2 -*geminal* dialkyl, the 1,3-substitution in 2,4-dpppt, also shows increased selectivity for O-allylation. A Newman projection cannot be used to explain loss of rotational freedom, but apparently for this complex also a more stable chelate is formed. However, in this case also the electronic environment on ruthenium is altered, making it impossible to point out the effect that is of highest importance for the higher selectivity.

3.2.7 Mechanistic implications

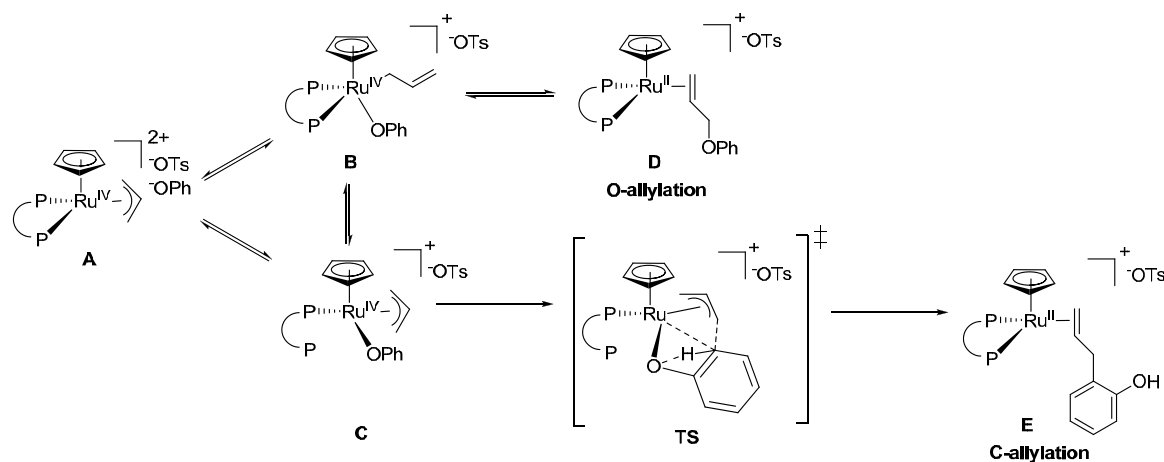
A catalytic cycle for the allylation of phenol with allyl alcohol catalyzed by ruthenium-Cp bidentate phosphine complexes has been proposed in Chapter 2. The oxidative addition of allyl alcohol in $[\text{Ru}(\text{II})\text{Cp}(\text{PP})(\text{allyl alcohol})](\text{OTs})$ followed by exchange of the hydroxyl with a phenolate group will produce the resting state $[\text{Ru}(\text{IV})\text{Cp}(\text{PP})(\pi\text{-allyl})](\text{OPh})(\text{OTs})$ (**A**) (Scheme 3.2). The phenolate anion, however, will be strongly attracted to the Ru(IV) ion in the dicationic complex. In order to prevent the formation of a 20-electron species, either the σ -allyl intermediate (**B**) is formed or a phosphine donor must dissociate (**C**). The route via the σ -allyl species is the analogous microscopic reverse of the oxidative addition of allyl alcohol (or ether) and will produce the O-allylated product allyl phenyl ether (**D**). When phosphine dissociation occurs, space is provided for the activation of the *ortho*-position of the phenyl

ring possibly via the transition state **TS** (Scheme 3.2) and C-allylated products can then be irreversibly formed (**E**).

The previous finding that [RuCp(dppm)](OTs) and [RuCp(dppe)](OTs) demonstrate a high selectivity to C-allylated product can now thus be interpreted as probably not due to the ample free coordination space at Ru due to the relatively small static bite angle of these diphosphine ligands, but rather to the ease of dissociation of one phosphine donor under allylation reaction conditions.

Generally, the catalysts containing *gem*-dialkyl substituted ligands are considerably less active for allylation of phenol than their unsubstituted analogues. This is in particular true in the absence of protic co-catalyst. Clearly, the oxidative addition of allyl alcohol is the rate-determining step in the overall catalytic cycle. Oxidative addition requires the penetration of the allyl alcohol (or allyl ether) substrate into the coordination sphere of the Ru(II) complex. It is thought that a kinetically stable chelate cannot easily provide sufficient coordination space to fulfill this requirement. In the ideal case, for high activity one would like to use flexible chelates during the oxidative addition step, such that allyl alcohol can easily penetrate the Ru(II) coordination sphere. However, for high selectivity kinetically stable chelation at the intermediate Ru(IV) center is required as is discussed above. These requirements seem conflicting.

Although the binding properties of the C_2 -geminal substituted C_3 ligands have been determined for the Ru(II) complexes and selectivity for O-allylation is controlled by a Ru(IV) species for which phosphines will have different binding strengths, it is concluded that the reduction of rotational freedom of the ligand must be the cause of the higher selectivity for O-allylation. Similarly, the high selectivity of [Ru(IV)Cp*(π -allyl)(acetonitrile) $_2$](PF $_6$) $_2$ catalyst



Scheme 3.2. Part of catalytic cycle for allylation with [RuCp(PP)](OTs) complexes where selectivity is determined.

precursors for C-allylation⁷ is rationalized to the rapid dissociation of the weakly-coordinating acetonitrile ligand. This is in contrast with the reported mechanistic proposal that C-allylation of phenol proceeds via an external electrophilic attack of phenol by the Ru- π -allyl species, without pre-coordination of phenol at the Ru(IV) center.⁷

The results provide a firm confirmation that the *gem*-dialkyl effect can serve as a diagnostic tool to probe possible chelate-ring opening in a catalytic reaction pathway, which in this case discriminates C-allylation vs O-allylation routes.

3.3 Conclusions

In the present research, a class of bidentate phosphine ligands that form kinetically stable chelates on ruthenium has been investigated for their use in the catalytic allylation of phenol. It is shown that this type of ligands has a highly beneficial effect on the selectivity of the ruthenium catalysts for O-allylation; the thermodynamically favored C-allylation can be efficiently blocked even after long reaction times. The cause of the kinetically stable chelating properties of these ligands is due to a reduced rotational freedom of the ligands. Therefore entropy gain on dissociation is low, which causes the ligand to remain coordinated onto ruthenium thus inducing high selectivity towards O-allylation. The rigidity of the ligand is also expected to hinder oxidative addition of allyl donors at Ru(II), which is considered to be the rate-determining step, explaining the relatively lower activity of complexes with C₂-*geminal* substituted C₃-bridging ligands. The *gem*-dialkyl effect is thus used both as diagnostic tool for detecting chelate-ring opening at the metal center in a selectivity-determining step of the catalytic cycle, and at the same time as a means to develop catalysts for the allylation of phenol with allyl alcohol with the desired high O-allylation selectivity.

3.4 Experimental

General remarks. All reactions were performed under an argon atmosphere using standard Schlenk techniques. Solvents were dried and distilled by standard procedures and stored under argon. The phosphine ligand (S,S)-2,3-dppb was commercially available and used as received. A modified protocol for the synthesis of the phosphine ligands was used.¹⁷ The ligands 2,2-dppp,¹⁸ dppdmp,¹⁹ dppdep,²⁰ dpptms,²¹ 2,4-dpppt,²⁰ dppib,²² and *o*-MeOdppdmp²³ were earlier described in literature. C, H determinations were performed on a Perkin Elmer 2400 Series II analyzer. ¹H NMR spectra (300 MHz), and ³¹P{¹H}NMR spectra (121.4 MHz) were measured on a Bruker DPX-300. Chemical shifts are reported in ppm. Proton chemical shifts are relative to TMS, and phosphorus chemical shifts are relative to 85% aqueous H₃PO₄. The spectra were taken at room temperature.

General procedure for ligand synthesis. HPPH₂ (1.0 ml, 6 mmol) was dissolved in THF (5 ml) and cooled to 0 °C. Butyl lithium (3.75 ml of a 1.6 M solution in hexanes) was added and the mixture was stirred at room temperature for 1 h. The appropriate dibromo-bridge was added (3 mmol) and the resulting solution was stirred for 16 h at room temperature. Water was added (10 ml) and the organic solvent was evaporated. The product was extracted with 3 times 10 ml of CH₂Cl₂, after which the organic layers were collected and the solvent was removed *in vacuo*. The product was precipitated from the remaining oil by addition of methanol.

General procedure for RuCpCl(PP) synthesis. A solution of RuCpCl(PPh₃)₂ (72 mg, 0.1 mmol) and the bidentate phosphine ligand (0.1 mmol) in 5 ml toluene was stirred for 16 h at 90 °C. The solution was cooled to room temperature and flushed over a column of silica gel (3 g, d = 1 cm) with 15 ml of toluene to remove triphenylphosphine. Finally, the orange product was eluted with ethyl acetate until the eluate was colorless. The solution was then concentrated *in vacuo* to approximately 1 ml and the product precipitated with petroleum ether.

[RuCpCl(dppdmp)] was obtained as a yellow solid in a yield of 54 mg (84%). Crystals suitable for X-ray diffraction were obtained by slow diffusion of n-hexane into a solution of the complex in toluene. Anal. Calcd for C₃₄H₃₅ClP₂Ru·0.33(toluene): C, 64.86; H, 5.64. Found: C, 64.64; H, 6.13. ¹H-NMR (CDCl₃): δ 7.63-7.49 (m, 8H, ArH), 7.35-7.26 (m, 12H, ArH), 4.48 (s, 5H, Cp), 3.02-2.95 (m, 2H, PCH), 2.17-2.10 (m, 2H, PCH), 1.02 (s, 3H, Me), 0.18 (s, 3H, Me). ³¹P{¹H}-NMR (CDCl₃): δ 40.0 (s).

[RuCpCl(dppdep)] was obtained as a yellow solid in a yield of 53 mg (79%). Crystals suitable for X-ray diffraction were obtained by slow diffusion of n-hexane into a solution of the complex in toluene. Anal. Calcd for C₃₆H₃₉ClP₂Ru·0.25(hexane)·0.25(water): C, 65.05; H, 6.28. Found: C, 64.61; H, 6.34. ¹H-NMR (CDCl₃): δ 7.67-7.61 (m, 4H, ArH), 7.51-7.45 (m, 4H, ArH), 7.37-7.30 (m, 12H, ArH), 4.39 (s, 5H, Cp), 2.87-2.79 (m, 2H, CH₂P), 2.18-2.09 (m, 2H, CH₂P), 1.25 (q, 2H, *J* = 7 Hz, CH₂), 0.71 (q, 2H, *J* = 7 Hz, CH₂), 0.64 (t, 3H, *J* = 7 Hz, CH₃), 0.14 (t, 3H, *J* = 7 Hz, CH₃). ³¹P{¹H}-NMR (CDCl₃): δ 39.6 (s).

[RuCpCl(*o*-MeOdppdmp)] was obtained as a yellow solid in a yield of 64 mg (84%). Crystals suitable for X-ray diffraction were obtained by slow diffusion of n-hexane into a solution of the complex in toluene. Anal. Calcd for C₃₈H₄₃ClO₄P₂Ru·1.5(toluene): C, 62.21; H, 5.91. Found: C, 62.20; H, 6.16. ¹H-NMR (CDCl₃): δ 7.37-7.12 (m, 8H, ArH), 7.03-6.93 (m, 7H, ArH), 6.69 (d, 4H, *J* = 8 Hz, ArH), 4.42 (s, 5H, Cp), 3.29 (s, 6H, OMe), 3.24 (s, 6H, OMe), 2.91-2.89 (m, 2H, CH₂), 2.62-2.60 (m, 2H, CH₂), 0.88 (s, 3H, Me), 0.25 (s, 3H, Me). ³¹P{¹H}-NMR (acetone-d₆): δ 38.1 (s).

[RuCpCl(dpptms)] was obtained as a yellow solid in a yield of 52 mg (81%). Crystals suitable for X-ray diffraction were obtained by slow diffusion of n-hexane into a solution of the complex in toluene. Anal. Calcd for C₃₃H₃₅ClP₂Ru·1.25(water): C, 60.73; H, 5.79. Found: C, 60.35; H, 5.84. ¹H-NMR (CDCl₃): δ 7.70-7.64 (m, 4H, ArH), 7.37-7.25 (m, 16H, ArH), 4.21 (s, 5H, Cp), 2.33-2.26 (m, 2H, PCH), 1.54-1.44 (m, 2H, PCH), -0.03 (s, 3H, Me), -0.38 (s, 3H, Me). ³¹P{¹H}-NMR (CDCl₃): δ 42.0 (s).

[RuCpCl(2,4-dpppt)] was obtained as a yellow solid in a yield of 70 mg (90%). Anal. Calcd for C₃₄H₃₅ClP₂Ru·0.25(hexane): C, 64.25; H, 5.85. Found: C, 64.23; H, 6.14. ¹H-NMR (CDCl₃): δ 7.85-7.82 (m, 4H, ArH), 7.37-7.34 (m, 8H, ArH), 7.27-7.20 (m, 8H, ArH), 4.13 (s, 5H, Cp), 3.23-3.16 (m, 2H, PCH), 2.03-1.81 (m, 2H, CH₂), 1.13 (bs, 6H, CH₃). ³¹P{¹H}-NMR (CDCl₃): δ 51.8 (s).

[RuCpCl(dppib)] was obtained as a yellow solid in a yield of 40 mg (92%). Anal. Calcd for $C_{33}H_{31}ClP_2Ru \cdot 0.33(\text{hexane})$: C, 64.20; H, 5.49. Found: C, 63.78; H, 5.87. 1H -NMR ($CDCl_3$): δ 7.76-7.71 (m, 4H, ArH), 7.36-7.35 (m, 8H, ArH), 7.26-7.10 (m, 8H, ArH), 4.68 (s, 2H, =CH₂), 4.42 (s, 5H, Cp), 3.68-3.59 (m, 2H, CH₂P), 3.22-3.12 (m, 2H, CH₂P). $^{31}P\{^1H\}$ -NMR ($CDCl_3$): δ 43.0 (s).

[RuCpCl(2,2-dppp)] was obtained as a yellow / orange solid in a yield of 61 mg (99%). Crystals suitable for X-ray diffraction were obtained by slow diffusion of n-hexane into a solution of the complex in toluene. Anal. Calcd for $C_{32}H_{31}ClP_2Ru \cdot 0.5(\text{toluene}) \cdot (\text{water})$: C, 62.88; H, 5.50. Found: C, 62.88; H, 5.98. 1H -NMR ($CDCl_3$): δ 7.95-7.89 (m, 4H, ArH), 7.50-7.33 (m, 16H, ArH), 4.52 (s, 5H, Cp), 1.73 (t, 3H, $J = 13$ Hz, CH₃), 1.26 (t, 3H, $J = 13$ Hz, CH₃). $^{31}P\{^1H\}$ -NMR ($CDCl_3$): δ 43.0 (s).

[RuCpCl({S,S}-2,3-dppb)] was obtained as a yellow solid in a yield of 60 mg (96%). Anal. Calcd for $C_{32}H_{31}ClP_2Ru \cdot 0.3(\text{toluene}) \cdot 0.3(\text{hexane})$: C, 65.22; H, 5.91. Found: C, 64.96; H, 6.18. 1H -NMR ($CDCl_3$): δ 7.91-7.87 (m, 2H, ArH), 7.64-7.41 (m, 9H, ArH), 7.31-7.23 (m, 4H, ArH), 7.11-7.05 (m, 2H, ArH), 4.30 (s, 5H, Cp), 2.68-2.62 (m, 1H, CH), 2.07-2.03 (m, 1H, CH), 1.01 (dd, 3H, $J = 7$ Hz, $J = 11$ Hz, CH₃), 0.80 (dd, 3H, $J = 7$ Hz, $J = 11$ Hz, CH₃). $^{31}P\{^1H\}$ -NMR ($CDCl_3$): δ 86.0 (d, $J = 41$ Hz), 64.5 (d, $J = 41$ Hz).

Table 3.6. Crystal data and structure refinement for the complexes [RuCpCl(dppdep)], [RuCpCl(dppdmp)], [RuCpCl(dpptms)], [RuCpCl(o-MeOdppdmp)] and [RuCpCl(2,2-dppp)]

	[RuCpCl (dppdep)]	[RuCpCl (dppdmp)]	[RuCpCl (dpptms)]	[RuCpCl(o- MeOdppdmp)]	[RuCpCl (2,2-dppp)]
formula	$C_{36}H_{39}ClP_2Ru \cdot \frac{1}{2}(C_7H_8)$	$C_{34}H_{35}ClP_2Ru$	$C_{33}H_{35}ClP_2RuSi$	$C_{38}H_{43}ClO_4P_2Ru$	$C_{32}H_{31}ClP_2Ru +$ unresolved solvent molecules
fw	716.20	642.08	658.16	762.18	614.03*
crystal form	yellow plate	orange plate	orange block	orange thick plate	orange plate
crystal size [mm ³]	0.35 × 0.17 × 0.06	0.35 × 0.21 × 0.06	0.30 × 0.25 × 0.23	0.23 × 0.18 × 0.07	0.37 × 0.20 × 0.10
crystal system	monoclinic	monoclinic	monoclinic	monoclinic	triclinic
space group	$P2_1/c$ (no. 14)	$P2_1/c$ (no. 14)	$P2_1/c$ (no. 14)	$P2_1/c$ (no. 14)	$P2_1/c$ (no. 14)
a [Å]	15.2270(6)	13.3991(9)	9.4136(4)	10.7944(3)	19.5137(1)
b [Å]	14.1527(8)	10.8631(7)	17.9105(7)	17.0749(2)	11.2169(3)
c [Å]	18.0689(7) Å	19.9844(9)	18.2181(9)	38.2828(4)	30.1980(15)
α [°]	-	-	-	-	-
β [°]	119.047(3)	96.917(2)	103.927(2)	96.808(1)	119.551(3) ^o
γ [Å ³]	-	-	-	-	-
V [Å ³]	3404.1(3)	2887.7(3)	2981.3(3)	7006.3(2)	5750.0(4)
Z	4	4	4	8	8
D _x [g/cm ³]	1.40	1.48	1.47	1.45	1.42*
μ [mm ⁻¹]	0.66	0.77	0.79	0.65	0.77*
abs. corr. method					
abs. corr. range	0.77–0.96	0.70–0.95	0.76–0.84	-	0.73–0.93
refl. (meas./unique)	42872/7807	47036/6637	41351/6839	100289/12389	67490/13221
param./restrain ts	427 /171	345/0	345/0	842/0	731/256
R1/wR2 [I>2 σ (I)]	0.0248/0.0514	0.0217/0.0511	0.0175/0.0420	0.0424/0.0863	0.0324/0.0711
R1/wR2 [all refl.]	0.0362/0.0551	0.0263/0.0532	0.0207/0.0436	0.0588/0.0931	0.0490/0.0761
S	1.022	1.052	1.098	1.081	1.048
$\rho_{\text{min/max}}$ [e/Å ³]	-0.44 - 0.42	-0.49 - 0.90	-0.30 - 0.35	-0.64 - 2.2	-0.52 - 0.52

[*]excluding the unresolved entity contribution

General procedure for catalytic reactions. 5 mmol of 4-*tert*-butylphenol (or in some experiments 4-*tert*-butylphenyl allyl ether), 0.005 mmol of the ruthenium complex, 0.01 mmol of AgOTs and, if indicated, 0.01 mmol of additive were charged into the reaction vessel and flushed with argon. Degassed and dried toluene was added (5 ml) and the mixture was stirred for five minutes. Allyl alcohol (or in some experiments *p*-cresol) was added (5-10 mmol) and the reaction was stirred at 100 °C. Samples were taken at certain time intervals with an airtight syringe and analyzed by gas chromatography (Chapter 2).

GLC method. Quantitative gas liquid chromatography analyses were carried out on a Varian CP-3800 apparatus equipped with a VF-1ms (25 m × 0.25 mm) column with decane as internal standard. The temperature gradient used was: isothermal for 5 minutes at 40 °C, heating 10 °C/minute to 250 °C and finally isothermal for 5 minutes at 250 °C.

X-ray crystallography. All reflection intensities were measured at 150(2) K using a Nonius KappaCCD diffractometer (sealed tube for compounds **a**, **b**, **c** and **d**, or rotating anode for compounds **e**, **f**, and **g**) with graphite-monochromated Mo $K\alpha$ radiation ($\lambda = 0.71073 \text{ \AA}$) under the program COLLECT.²⁴ The programs PEAKREF²⁵ or HKL2000²⁶ were used to refine cell dimensions. Data were reduced using the integration programs EvalCCD²⁷ or HKL2000.²⁶ All structures were solved with DIRDIF99²⁸ or SHELXS-97 and were refined on F^2 with SHELXL-97.²⁹ Multi-scan semi-empirical absorption corrections based on symmetry-related measurements were applied to all data (except for [RuCpCl(*o*-MeOdppdmp)]) using SADABS (Version 2006/1)³⁰ or TWINABS Version 1.05.³¹ The data collection temperature was controlled using the system Oxford Cryostream 600 (manufactured by Oxford Cryosystems). The H-atoms (except when specified) were placed at calculated positions (instructions AFIX 23, 43 or 137) with isotropic displacement parameters having values 1.2 or 1.5 times U_{eq} of the attached C atoms, and were refined with a riding model. Geometry calculations, structure validations and illustrations were made with the PLATON program.³² For [RuCpCl(*o*-MeOdppdmp)]: The crystal that was mounted on the diffractometer was not single but rather an aggregate of two single crystals stuck in an arbitrary arrangement. The program DIRAX³³ found the two orientations matrices. The fractional contribution of the minor component (*i.e.*, the BASF batch scale factor) refined to 0.1520(10). For [RuCpCl(2,2-dppp)]: SQUEEZE details: two voids of 152 \AA^3 filled with 32 electrons (all numbers are given per unit cell). Relevant crystal structure and refinement data are provided in Table 3.6.

3.5 References

- (1) Au, A. T.; Nafziger, J. L. *Patent* **1996**, WO 9620232.
- (2) Bruneau, C.; Renaud, J. L.; Demerseman, B. *Chem.-Eur. J.* **2006**, *12*, 5178-5187.
- (3) Zhang, H. J.; Demerseman, B.; Xi, Z. F.; Bruneau, C. *Eur. J. Inorg. Chem.* **2008**, 3212-3217.
- (4) Onitsuka, K.; Okuda, H.; Sasai, H. *Angew. Chem.-Int. Edit.* **2008**, *47*, 1454-1457.
- (5) Satoh, T.; Ikeda, M.; Miura, M.; Nomura, M. *J. Org. Chem.* **1997**, *62*, 4877-4879.
- (6) Tada, Y.; Satake, A.; Shimizu, I.; Yamamoto, A. *Chem. Lett.* **1996**, 1021-1022.
- (7) Nieves, I. F.; Schott, D.; Gruber, S.; Pregosin, P. S. *Helv. Chim. Acta* **2007**, *90*, 271-276.
- (8) Bruce, M. I.; Wong, F. S.; Skelton, B. W.; White, A. H. *J. Chem. Soc.-Dalton Trans.* **1981**, 1398-1405.
- (9) Pearson, W. H.; Shade, J. E.; Brown, J. E.; Bitterwolf, T. E. *Acta Crystallogr. Sect. C-Cryst. Struct. Commun.* **1996**, *52*, 1106-1110.
- (10) Alonso, A. G.; Reventos, L. B. *J. Organomet. Chem.* **1988**, *338*, 249-254.
- (11) Bruce, M. I.; Ellis, B. G.; Low, P. J.; Skelton, B. W.; White, A. H. *Organometallics* **2003**, *22*, 3184-3198.

- (12) van der Drift, R. C.; Bouwman, E.; Drent, E.; Kooijman, H.; Spek, A. L.; van Oort, A. B.; Mul, W. P. *Organometallics* **2002**, *21*, 3401-3407.
- (13) van Rijn, J. A.; Marques-Gallego, P.; Reedijk, J.; Lutz, M.; Spek, A. L.; Bouwman, E. *Dalton Trans.* **2009**, 10727-10730.
- (14) Marcone, J. E.; Moloy, K. G. *J. Am. Chem. Soc.* **1998**, *120*, 8527-8528.
- (15) Arthur, K. L.; Wang, Q. L.; Bregel, D. M.; Smythe, N. A.; O'Neill, B. A.; Goldberg, K. I.; Moloy, K. G. *Organometallics* **2005**, *24*, 4624-4628.
- (16) Mul, W. P.; van der Made, A. W.; Smaardijk, A. A.; Drent, E. In *Catalytic Synthesis of Alkene-carbon monoxide copolymers and cooligomers*; Sen, A., Ed.; Kluwer Academic Publishers: Dordrecht, 2003, p 87-140.
- (17) Hewertson, W.; Watson, H. R. *J. Chem. Soc.* **1962**, 1490-&.
- (18) Pons, A.; Rossell, O.; Seco, M.; Solans, X.; FontBardia, M. *J. Organomet. Chem.* **1996**, *514*, 177-182.
- (19) Kraihanzel, C. S.; Ressler, J. M.; Gray, G. M. *Inorg. Chem.* **1982**, *21*, 879-887.
- (20) Bianchini, C.; Lee, H. M.; Meli, A.; Moneti, S.; Vizza, F.; Fontani, M.; Zanello, P. *Macromolecules* **1999**, *32*, 4183-4193.
- (21) de Groot, D.; Reek, J. N. H.; Kamer, P. C. J.; van Leeuwen, P. *Eur. J. Org. Chem.* **2002**, 1085-1095.
- (22) Schmidbaur, H.; Paschalidis, C.; Steigelmann, O.; Muller, G. *Chem. Berichte* **1989**, *122*, 1851-1855.
- (23) Ginkel, R. v.; Made, A. v. d.; With, J. d.; Eilenberg, W. *Patent* **2003**, *US 6548708B1*.
- (24) *Nonius. COLLECT 1999, Nonius BV*, Delft, The Netherlands.
- (25) Schreurs, A. M. M. *PEAKREF 1999*, University of Utrecht: The Netherlands.
- (26) Otwinowski, Z.; Minor, W. *Processing of X-ray Diffraction Data Collected in Oscillation Mode Methods in Enzymology*, C.W. Carter, Jr. & R. M. Sweet, Eds. **1997**, Volume 276: *Macromolecular Crystallography, part A*, 307-326.
- (27) Duisenberg, A. J. M.; Kroon-Batenburg, L. M. J.; Schreurs, A. M. M. *J. Appl. Crystallogr.* **2003**, *36*, 220-229.
- (28) Beurkens, P. T.; Admiraal, G.; Beurkens, G.; Bosman, W. P.; Garcia-Granda, S.; Gould, R. O.; Smits, J. M. M.; C., S. *The DIRDIF99 program system, Technical Report of the Crystallography Laboratory at University of Nijmegen* University of Nijmegen: Nijmegen, The Netherlands, 1999.
- (29) Sheldrick, G. M. *Acta Crystallogr.* **2008**, *A64*, 112-122.
- (30) Sheldrick, G. M. In *SADABS, Version 2006/1* University of Göttingen, Germany, 2006.
- (31) Sheldrick, G. M. In *TWINABS, Version 1.05* University of Göttingen, Germany, 2003.
- (32) Spek, A. L. *J. Appl. Crystallogr.* **2003**, *36*, 7-13.
- (33) Duisenberg, A. J. M. *J. Appl. Crystallogr.* **1992**, *25*, 92-96.